Some Historical Remarks on Mixed and Reduced and Selective Integration Methods

Mixed finite element formulations were first discussed by Fraeijs de Veubeke [42] and Herrmann [43]. Herrmann developed a reduced form of Reissner's variational principle particularly suited to problems of incompressible and nearly incompressible elasticity and, based upon this principle, established the first effective finite elements for such cases. This is the formulation given in Sec. 4.3. Prior to this development many displacement models were applied to these problems, and poor behavior was typically observed. The reasons for this were not understood at the time. Certain elements derived from Herrmann's formulation also failed. Hughes and Allik [39] traced this failure to a correspondence between mixed and displacement models, contained within Fraeijs de Veubeke's ***limitation principle*** [42].

The first example of a uniform reduced integration element was apparently the plate-shell element presented by Zienkiewicz et al. [44]. This element, among others, is discussed in Chapter 5. The same concept was employed in other areas by Zienkiewicz and colleagues. In particular, Naylor [45] and Zienkiewicz and Godbole [46] advocated the use of the eight-node serendipity element in problems involving incompressibility. The procedure, however, was viewed by many as more a "trick" than a method and some bad experiences were subsequently noted for the serendipity element.

The concept of selective integration was first employed by Doherty et al. [47] to obtain improved bending behavior in simple four-node elasticity elements. One-point Gauss quadrature was used on the shear-strain term, and 2×2 Gauss quadrature was used to integrate the remaining terms. Although improved behavior was noted in some configurations, lack of invariance opened the approach to criticism.

Studies performed by Fried [38], Nagtegaal et al. [40], and Argyris et al. [48] provided fresh insights into why the displacement approach failed in constrained problems. Malkus [49, 50] proved the equivalence of a class of mixed models with reduced selective integration single-field elements in linear elasticity theory. The equivalence results of Malkus and Hughes [36] elevated the reduced and selective integration approaches from the realm of tricks to a legitimate methodology. Considerable research on the behavior of mixed and reduced and selective integration elements has taken place in recent years. A summary of more recent developments is contained in the following sections.

4.4.1 Pressure Smoothing

The pressure field in the reduced and selective integration penalty function formulation is to be viewed as discontinuous from element to element. In fact, all displacement derivatives for C^0 isoparametric elements are, in general, discontinuous across element boundaries. Thus, for plotting purposes, it is desirable to employ a smoothing procedure, which redefines the field under consideration in terms of the displacement shape functions N_A.

With specific reference to the pressure, there is at least one other reason for employing a smoothing procedure. It was mentioned earlier that, in certain situations,

discontinuous-pressure, mixed-method finite elements exhibit a rank-deficiency in the assembled pressure equations. By the equivalence theorem, "problems" are also to be expected with the pressure field of the penalty function formulation. These problems typically manifest themselves as pressure oscillations. For example, if four-node, quadrilateral elements are employed in a square mesh, with an even number of square elements in each direction, subjected to all velocity boundary conditions, then a checkerboard pressure oscillation is produced. Despite the pressure oscillations, the velocity field remains good.

Fortunately, smoothing procedures of a ***least squares*** type [51] seem to perform the necessary filtering as a byproduct. A comprehensive study of such techniques has been performed by Lee et al. [52]. The methods we prefer for constant-pressure elements [53], which involve slight modifications of schemes proposed in [52], are described next.

Let the discontinuous pressure field be written as

$$p^h = \sum_{e=1}^{n_{el}} \psi^e p^e \tag{4.4.25}$$

where p^e is the element mean pressure and ψ^e is the eth element "characteristic function," i.e.,

$$\psi^e(\boldsymbol{x}) = \begin{cases} 1 & \text{if } \boldsymbol{x} \in \Omega^e \\ 0 & \text{if } \boldsymbol{x} \notin \Omega^e \end{cases} \tag{4.4.26}$$

The smoothed pressure is written

$$\widetilde{p} = \sum_{A=1}^{n_{np}} N_A \widetilde{p}_A \tag{4.4.27}$$

The standard least squares procedure gives rise to the following matrix problem:[7]

$$\boldsymbol{Y}\widetilde{\boldsymbol{p}} = \boldsymbol{P} \tag{4.4.28}$$

where

$$\boldsymbol{Y} = [Y_{AB}] \tag{4.4.29}$$

$$\widetilde{\boldsymbol{p}} = \{\widetilde{p}_B\} \tag{4.4.30}$$

and

$$\boldsymbol{P} = \{P_A\} \tag{4.4.31}$$

[7] The least squares procedure defines $\widetilde{p}$ by minimizing

$$\int_\Omega (\widetilde{p} - p^h)^2 \, d\Omega$$

with respect to the $\widetilde{p}_A$'s. The resulting equations emanate from

$$\frac{\partial}{\partial \widetilde{p}_A} \int_\Omega (\widetilde{p} - p^h)^2 \, d\Omega = 0$$

for $A = 1, 2, \ldots, n_{np}$.

The indices A, B take on the values $1, 2, \ldots, n_{np}$. The construction of $\boldsymbol{Y}$ and $\boldsymbol{P}$ is performed in the usual element-by-element fashion, viz.[8]

$$\boldsymbol{Y} = \mathop{\mathbf{A}}_{e=1}^{n_{el}} (y^e), \qquad \boldsymbol{P} = \mathop{\mathbf{A}}_{e=1}^{n_{el}} (p^e) \tag{4.4.32}$$

in which

$$y^e = [y^e_{ab}], \qquad p^e = \{p^e_a\}, \qquad 1 \le a,\ b \le n_{en} \tag{4.4.33}$$

$$y^e_{ab} = \int_{\Omega^e} N^e_a N^e_b \, d\Omega, \qquad p^e_a = p^e \int_{\Omega^e} N^e_a \, d\Omega \tag{4.4.34}$$

As it stands, the matrix $\boldsymbol{Y}$ is symmetric and positive-definite and possesses a band-profile structure. Additional simplification may be engendered by replacing $\boldsymbol{Y}$ by an associated diagonal matrix.[9] This is done by approximating the first of (4.4.34); effective procedures are summarized as follows:

$n = 2$; rectilinear case. The 2×2 product, trapezoidal integration rule may be used to diagonalize y^e, i.e.,

$$y^e_{ab} = \delta_{ab} j^e(\xi_a, \eta_a) \qquad \text{(no sum on } a\text{)} \tag{4.4.35}$$

where

$$j^e = \det \begin{bmatrix} x^e_{1,\xi} & x^e_{1,\eta} \\ x^e_{2,\xi} & x^e_{2,\eta} \end{bmatrix} \qquad \text{(Jacobian determinant)} \tag{4.4.36}$$

$$\boldsymbol{x}^e = \sum_{a=1}^{n_{en}} N^e_a \boldsymbol{x}^e_a \tag{4.4.37}$$

and ξ_a and η_a are the coordinates of node a in the element "natural" coordinate system. Applying the same integration scheme to the second of (4.4.34) yields

$$p^e_a = p^e j^e(\xi_a, \eta_a) \tag{4.4.38}$$

Further simplification may be achieved by approximating $j^e(\xi_a, \eta_a)$ in (4.4.35) and (4.4.38) by $j^e(0, 0)$. (When Ω^e is a parallelogram, j^e is constant and no loss of accuracy is incurred by this procedure.)

The three-dimensional case is the straightforward generalization of the above, so we omit the details.

$n = 2$; axisymmetric case. If we attempt to apply the above procedure in the axisymmetric case, we encounter a difficulty due to the factor x_1 (i.e., r) in the integrands. Along the x_2-axis, $x_1 = 0$; hence the trapezoidal integration technique will

[8] The "assembly operators" in (4.4.32) are not the same as those used previously. Here, no boundary conditions are taken account of and there is only one degree of freedom per node.

[9] Lee et al. [52] have also found that higher accuracy is attained when $\boldsymbol{Y}$ is diagonal!

produce a zero diagonal entry in $\boldsymbol{Y}$. In this case we employ a "row-sum" diagonalization technique in which

$$y^e_{ab} = \delta_{ab} \int_{\Omega^e} N^e_a \, d\Omega \qquad \text{(no sum on } a\text{)} \tag{4.4.39}$$

The above integration, which also suffices for the second of (4.4.34), may be performed by either one-point or 2×2 Gauss-Legendre integration—the latter scheme being exact.

The procedures just described render the formation, storage, and solution of the matrix equation (4.4.28) very efficient. The results produced tend to be very good at interior nodes but leave something to be desired at boundary nodes. To improve upon the results, a "correction" at each boundary node is performed. The procedure used for four-node elements may be described with the aid of an example.

Consider the mesh illustrated in Fig. 4.4.5(a). The nodes are segregated into four groups. The boundary node corrections are carried out in the following steps in order:

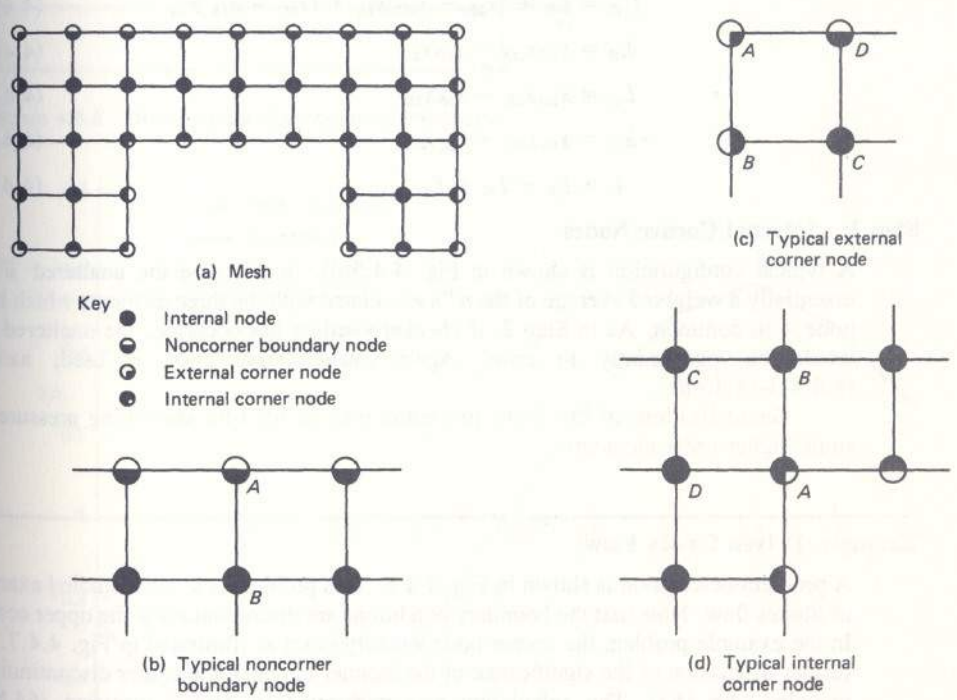

Figure 4.4.5 Example mesh for four-node element, pressure-smoothing algorithm.

Step 1: Noncorner, Boundary Nodes

A typical case of a noncorner, boundary node is depicted in Fig. 4.4.5(b). It may be observed that the unaltered value of $\tilde{p}_A$ is actually a higher-order approximation to the

pressure at the midpoint of the line joining nodes A and B; see Barlow [54]. Thus we redefine the $\tilde{p}_A$ by way of linear extrapolation, i.e.,

$$\tilde{p}_A \longleftarrow 2\tilde{p}_A - \tilde{p}_B \tag{4.4.40}$$

Step 2: External Corner Nodes

A typical situation is depicted in Fig. 4.4.5(c). The unaltered value of $\tilde{p}_A$ is precisely the constant pressure p^e, because the above procedures reduce to "do-nothing" calculations at external corners. (If checkerboarding was occuring in the p^e's, the value of $\tilde{p}_A$ would be grossly in error.) In this case linear extrapolation is employed through nodes B, C, and D, i.e.,

$$\tilde{p}_A \longleftarrow \frac{\tilde{L}_B\tilde{p}_B + \tilde{L}_C\tilde{p}_C + \tilde{L}_D\tilde{p}_D}{L} \tag{4.4.41}$$

where

$$\tilde{L}_B = L_B + (x_{2C} - x_{2D})x_{1A} + (x_{1D} - x_{1C})x_{2A} \tag{4.4.42}$$

$$\tilde{L}_C = L_C + (x_{2D} - x_{2B})x_{1A} + (x_{1B} - x_{1D})x_{2A} \tag{4.4.43}$$

$$\tilde{L}_D = L_D + (x_{2B} - x_{2C})x_{1A} + (x_{1C} - x_{1B})x_{2A} \tag{4.4.44}$$

$$L_B = x_{1C}x_{2D} - x_{1D}x_{2C} \tag{4.4.45}$$

$$L_C = x_{1D}x_{2B} - x_{1B}x_{2D} \tag{4.4.46}$$

$$L_D = x_{1B}x_{2C} - x_{1C}x_{2B} \tag{4.4.47}$$

$$L = L_B + L_C + L_D \tag{4.4.48}$$

Step 3: Internal Corner Nodes

A typical configuration is shown in Fig. 4.4.5(d). In this case the unaltered $\tilde{p}_A$ is essentially a weighted average of the p^e's associated with the three elements which have node A in common. As in Step 2, if checkerboarding has occurred, the unaltered $\tilde{p}_A$ would be significantly in error. Again linear extrapolation is used; namely (4.4.41)–(4.4.48).

Generalizations of the above procedure may be used for smoothing pressures in some higher-order elements.

Example (Driven Cavity Flow)

A problem description is shown in Fig. 4.4.6. This problem is a much studied example of Stokes flow. Note that the boundary conditions are discontinuous at the upper corner. In the example problem the corner node velocity is set as illustrated in Fig. 4.4.7. For further discussion of the significance of the manner in which the corner discontinuity is modeled, see [53]. The calculation was performed in double precision (64 bits/floating-point word). The penalty parameter was defined by $\lambda/\mu = 10^7$. A 10×10 mesh of bilinear elements was employed with the $S1$ integration scheme. The unsmoothed pressures exhibit significant oscillations, which are removed by the method described above; see Fig. 4.4.8.

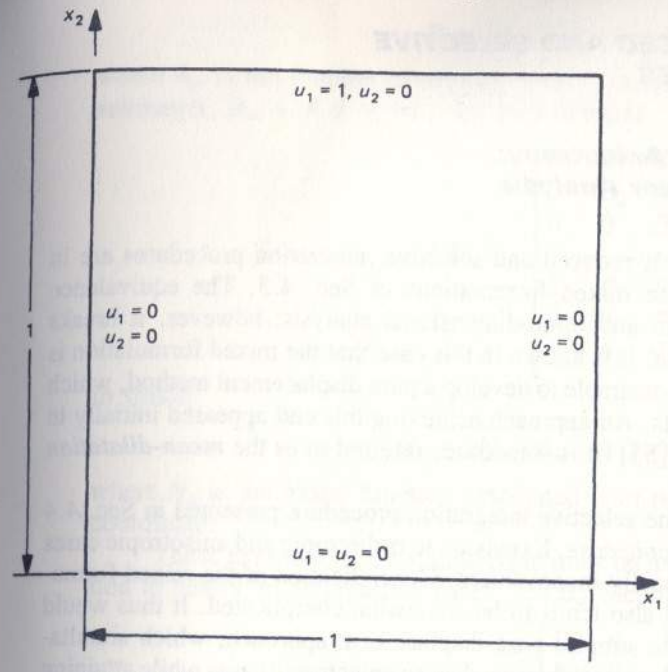

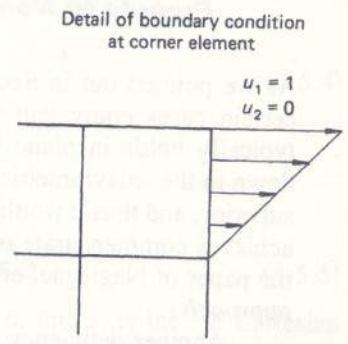

Figure 4.4.7

Figure 4.4.6 Driven cavity flow: problem description.

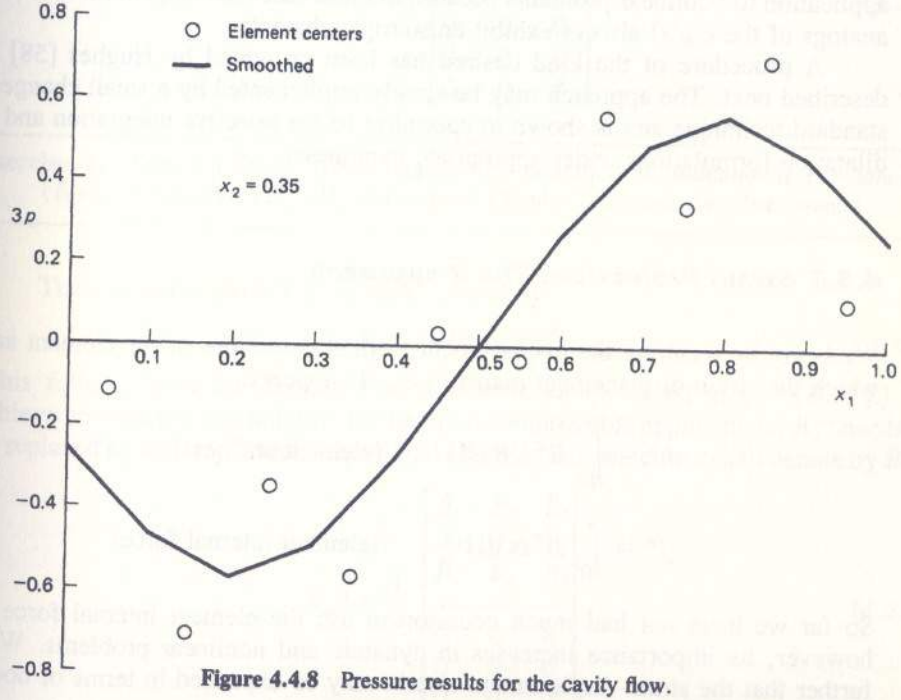

Figure 4.4.8 Pressure results for the cavity flow.